Cell, Vol. 122, 235–246, July 29, 2005, Copyright ©2005 by Elsevier Inc. DOI 10.1016/j.cell.2005.05.032

Transcriptional Feedback of *Neurospora* Circadian Clock Gene by Phosphorylation-Dependent Inactivation of Its Transcription Factor

Tobias Schafmeier,[1] Andrea Haase,[1] Krisztina Káldi,[1] Johanna Scholz, Marc Fuchs, and Michael Brunner*
Biochemistry Center
University of Heidelberg
Im Neuenheimer Feld 328
D-69120 Heidelberg
Germany

Summary

The circadian clock protein Frequency (FRQ) feedback-regulates its own expression by inhibiting its transcriptional activator, White Collar Complex (WCC). We present evidence that FRQ regulates the bulk of WCC through modulation of its phosphorylation status rather than via direct complex formation. In the absence of FRQ, WCC is hypophosphorylated and transcriptionally active, while WCC is hyperphosphorylated and transcriptionally inactive when FRQ is expressed. The phosphorylation status of WCC changes rhythmically over a circadian cycle. Dephosphorylation and activation of WCC depend on protein phosphatase 2A (PP2A), and WCC is a substrate of PP2A in vitro. Hypophosphorylated WCC binds to the clock box of the *frq* promoter even in the presence of FRQ, while binding of hyperphosphorylated WCC is compromised even when FRQ is depleted. We propose that negative feedback in the circadian clock of *Neurospora* is mediated by FRQ, which rhythmically promotes phosphorylation of WCC, functionally equivalent to a cyclin recruiting cyclin-dependent kinase to its targets.

Introduction

Circadian clocks are self-sustained cellular oscillators that organize temporal expression of a large number of genes in many organisms. By synchronizing to the solar light cycle, circadian oscillations achieve a precise 24 hr period, while the periodicity is ~24 hr in the absence of environmental cues. A negative transcriptional/translational feedback loop, interconnected with positive and negative regulatory loops, constitutes the core of circadian clocks in fungi, plants, and animals. Phosphorylation and posttranscriptional control mechanisms regulate rhythmic subcellular distribution and turnover kinetics of clock components and are crucial for period length and robust rhythmicity (Dunlap 1999; Allada et al., 2001; Young and Kay, 2001; Reppert and Weaver, 2002; Schibler and Sassone-Corsi, 2002; Roenneberg and Merrow, 2003; Stanewsky, 2003; Gachon et al., 2004).

Here we have addressed the molecular mechanism of negative feedback of the *Neurospora* clock protein FRQ on expression of its own RNA. Rhythmic transcription of *frq* is essential for circadian rhythmicity (Aronson et al., 1994a). *frq* transcription is activated by the White Collar Complex (WCC), a hetero-oligomer containing the PAS-domain transcription factors WC-1 and WC-2 (Linden and Macino, 1997; Froehlich et al., 2002; Froehlich et al., 2003). WCC binds to two light-responsive elements in the *frq* promoter (Froehlich et al., 2002). The distal element, the clock box (C box), is necessary and sufficient for rhythmic expression of *frq* RNA in constant darkness (Froehlich et al., 2003). When FRQ protein is expressed, binding of WCC to the C box is compromised (Froehlich et al., 2003), resulting in reduction of *frq* RNA levels (Aronson et al. 1994a). Previously synthesized FRQ is degraded and active WCC emerges again, initiating a new circadian cycle. FRQ also participates in positive regulation, supporting expression of WC-1 and WC-2 (Lee et al., 2000; Cheng et al., 2001; 2003; Merrow et al., 2001). In constant darkness, the negative and positive feedback loops lead to robust self-sustained circadian oscillation in *frq* RNA and FRQ protein amount with a period of ~22 hr at 25°C. Period, phase, and amplitude of oscillations of *frq* and FRQ abundance are regulated by a number of protein kinases and protein phosphatases (PP). CKI, CKII, and CAMK-1 affect FRQ stability (Görl et al., 2001; Yang et al., 2001; Yang et al., 2002; Yang et al., 2003). Similarly, PP1 regulates FRQ turnover (Yang et al., 2004). PP2A is a trimer of a catalytic (C), a structural (A), and a regulatory subunit (Virshup, 2000). Inactivation of *rgb-1*, one regulatory subunit of PP2A, results in a severe growth defect (Yatzkan and Yarden, 1999), reduced expression of FRQ, and altered circadian rhythmicity (Yang et al., 2004).

WC-1 contains a flavin binding LOV domain (Froehlich et al., 2002; He et al., 2002). It acts as blue-light receptor for photoperiodic entrainment and resetting of the clock. Its activation by light is accompanied by transient phosphorylation and subsequent degradation (Talora et al., 1999; Schwerdtfeger and Linden, 2000; Lee et al., 2003). In constant light, overall WCC activity is increased and *frq* RNA and FRQ protein are constitutively expressed at elevated levels. WC-1 is also phosphorylated in constant darkness at sites distinct from the light-dependent phosphorylation sites (He et al. 2005).

The central pacemaker drives rhythmic expression of a large number of clock-controlled genes (Bell-Pedersen et al., 1996; Zhu et al., 2001; Correa et al., 2003; Nowrousian et al., 2003).

FRQ was found in a complex with the RNA helicase FRH (Cheng et al. 2005), a putative component of the exosome complex that mediates 3′ to 5′ trimming of many RNA species, including mRNA. The functional significance of this association is not yet understood.

WCC is concentrated in the nucleus (Schwerdtfeger and Linden, 2000), while the localization of FRQ is predominantly cytosolic, and the bulk of WCC does not interact with FRQ (Cheng et al. 2005). We show that WCC is expressed in excess over nuclear FRQ, excluding that WCC is directly inactivated by complex formation with FRQ. Rather, FRQ directly or indirectly controls the phosphorylation state of WCC. In contrast to light-dependent phosphorylation, FRQ-dependent phosphory-

*Correspondence: michael.brunner@urz.uni-heidelberg.de
[1]These authors contributed equally to this work.

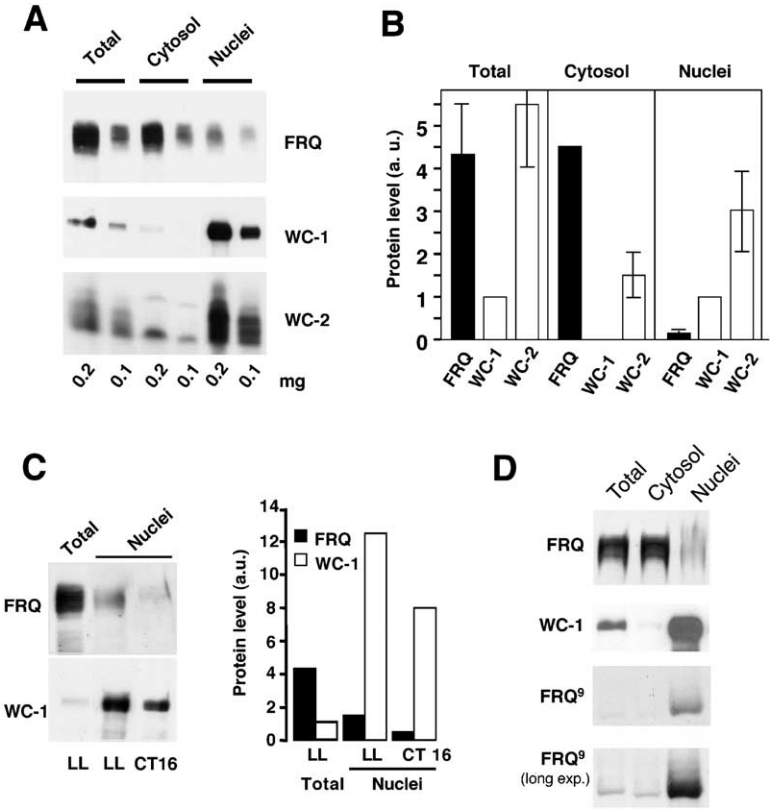

Figure 1. Subcellular Distribution and Quantification of FRQ, WC-1, and WC-2

(A) Total protein extract from light-grown *Neurospora* was fractionated into cytosol and nuclei. Indicated amounts of protein were analyzed by SDS-PAGE and immunoblotting with antibodies against FRQ, WC-1, and WC-2.

(B) Relative abundance of clock proteins in subcellular compartments. Calibration curves with radiolabeled clock proteins (Figure S1) were used to convert Western blot signals (FluorS-Max) of FRQ, WC-1, and WC-2 into mole equivalents. WC-1 abundance in total extract and in nuclei was set equal to 1. (WC-1 was not quantified in the cytosolic fraction.) Columns represent the average of 3 to 5 experiments with duplicate samples. (Error bars: ± SD.)

(C) Relative concentration of FRQ and WC-1 in nuclei. Left panel: Aliquots of total cell extract and nuclei from light-grown *Neurospora* and nuclei prepared at ~CT16 (DD25) were analyzed. Right panel: Molar ratio of FRQ and WC-1 was determined. Values are expressed relative to WC-1 abundance in total extract (LL), which was set equal to 1.

(D) The C-terminally truncated mutant FRQ^9 protein is enriched in nuclei. Subcellular fractions from frq^+ and frq^9 were analyzed with the indicated antibodies. Right panels: frq^+; left panels: frq^9. A longer exposure is shown in the bottom panel to compare FRQ^9 in total extract and cytosol.

lation of WCC correlates with its inactivation and reduction of *frq* RNA levels in vivo. Hypophosphorylated WCC, on the other hand, supports expression of *frq* RNA. Rhythmic transcription of *frq* correlates with changes in the phosphorylation status of WCC. Dephosphorylation of WCC in vivo is dependent on the PP2A regulatory subunit RGB-1 and is accompanied by an increase in *frq* RNA levels. In vitro, purified WCC is dephosphorylated by PP2A. Hypophosphorylated WCC binds efficiently to a C box oligonucleotide derived from the *frq* promoter, while hyperphosphorylated WCC binds with reduced affinity. In summary, in vitro and in vivo evidence suggests that FRQ inactivates WCC by promoting its phosphorylation. Recruitment by dephosphorylation of a relatively small fraction of active WCC primarily from a large pool of inactive protein rather than by de novo synthesis may contribute to the robustness of the circadian oscillator.

Results

Subcellular Distribution of Clock Proteins

Light-grown *Neurospora* (*bd*) was fractionated, and aliquots of total, cytosolic, and nuclear fractions were analyzed by Western blotting (Figure 1A). The concentration of FRQ in the cytosolic fraction was indistinguishable from its concentration in total cell extract. Approximately 95% of FRQ was localized in the cytosol, supporting recent findings that the vast majority of FRQ was localized in the cytoplasm (Cheng et al. 2005). In contrast, WC-1 and WC-2 were highly enriched in nuclei (Figure 1A). As reported previously, ~1/3 of WC-2 was localized in the cytosol, and nuclear forms of WC-2 displayed reduced electrophoretic mobility due to compartment-specific phosphorylation (Schwerdtfeger and Linden, 2000).

WC-1 is a marker for WCC since it does not accumulate in the absence of its assembly partner WC-2 (Cheng et al., 2002). FRQ and WCC (WC-1) are expressed in similar amounts (Denault et al. 2001). However, as shown above, the vast majority of FRQ is localized in the cytoplasm, while WCC is localized in nuclei. We determined the stoichiometric relationship of clock proteins in cytosol and nuclei (Figure 1B and Figure S1) using in vitro-synthesized radiolabeled clock proteins for calibration (Denault et al., 2001). For an initial quantification, light-grown *Neurospora* (LL) was used since FRQ is constitutively expressed at elevated levels under these conditions. In total extracts, the molar ratio of FRQ versus WCC (WC-1) was 4.3:1 (Figure 1B, left panel). In nuclei, however, WCC was present in ~7-fold excess over nuclear FRQ (Figure 1B, right panel).

In constant darkness (DD), *frq* RNA oscillates in amount, reaching a maximum 4 hr after subjective dawn at circadian time 4 (CT4 ~DD15) and a minimum around CT15–17 (~DD25), i.e., 3–5 hr after subjective dusk. *Neurospora* was grown for 25 hr in DD (CT16), and nuclei were analyzed (Figure 1C). The molar ratio of nuclear FRQ versus WC-1 was ~1:15. Thus, under conditions where *frq* RNA synthesis is maximally repressed, WCC is present in large excess over nuclear FRQ.

For the analysis shown above, the integrity of nuclei is crucial. Several lines of evidence demonstrate that the cytosolic localization of FRQ is not an artifact due to damaged or perforated nuclei. Namely, the distinct phosphorylation patterns of nuclear and cytosolic WC-2 and the absence of WC-1 in the cytosolic fraction indicate that nuclei remained mostly intact during the preparation. Furthermore, we noticed that the C-terminally truncated, mutant FRQ^9 protein (Aronson et al., 1994b), though expressed at low levels, is highly enriched in nuclear fractions (Figure 1D). This internal control supports that the cytosolic localization of full-size FRQ was not due to preparation artifacts.

Interaction of Clock Proteins

To determine whether FRQ interacts with WCC, nuclear and total extracts (LL) were analyzed by gel filtration (Figure 2A and Figure S2A). FRQ and WCC (WC-1) eluted in separate fractions with minimal overlap, corresponding to an apparent molecular mass (app. M_r) of about 700 kDa and 450 kDa, respectively. An additional peak corresponding to a complex of FRQ and WCC (expected M_r ~700 kDa + 450 kDa) was not detected, supporting that the majority of WCC did not stably interact with FRQ and vice versa. The elution profiles of the clock components did not change when nuclear extract from dark-grown *Neurospora* was analyzed but the levels of FRQ were lower (not shown). Corresponding results were obtained by sucrose-density-gradient centrifugation (Denault et al., 2001 and data not shown), although the app. M_rs of FRQ and WCC were consistently about half of those determined by gel filtration.

We then prepared total cell extract (DD25) and performed immunoprecipitation. When WC-1 was immunodepleted, a small amount of FRQ was coimmunoprecipitated (Figure 2B). However, the fraction of FRQ in complex with WCC corresponded to only ~1.5%, while the vast majority of FRQ was not associated with WCC. Similarly, only a minor fraction of WC-1 coimmunoprecipitated with FRQ (Figure S2B), confirming recent reports that only a small fraction of FRQ is associated with WCC (Cheng et al. 2005). This small fraction could represent a subpopulation of WCC that is transiently associated with FRQ.

In summary, subcellular localization studies, quantification, gel filtration analysis, as well as immunoprecipitation demonstrate quantitatively and qualitatively that WCC is present in excess over FRQ in the nucleus and that the vast majority of WCC is not associated with FRQ. This raises the question of how FRQ feeds back on WCC to inhibit synthesis of its own RNA. Obviously, FRQ could neutralize only a very small fraction of WCC by binding in a stoichiometric complex. Thus, FRQ may trigger inactivation of an excess of WCC by catalytic means.

FRQ-Dependent Phosphorylation of WCC

Analysis of nuclear fractions indicated that WC-1 and WC-2 were phosphorylated in constant conditions (Figure S3; Lee et al., 2000; Schwerdtfeger and Linden, 2000). To investigate whether FRQ affects the phosphorylation status of WCC, we analyzed nuclear fractions of two *frq*-deficient strains. In frq^{10}, the *frq* gene

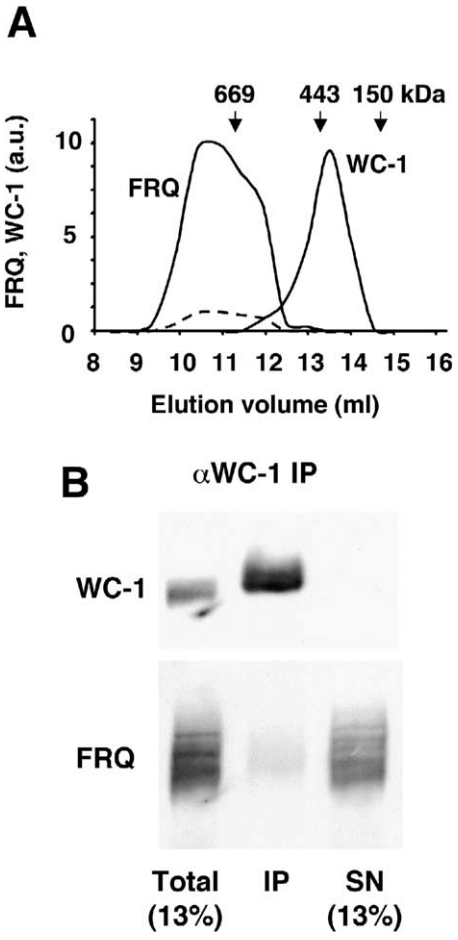

Figure 2. The Majority of WCC Does Not Stably Interact with FRQ

(A) Nuclear extract was subjected to gel filtration chromatography (Superose 6). Fractions (0.5 ml) were collected and aliquots were analyzed by SDS-PAGE and immunoblotting with antibodies against FRQ and WC-1. Signals were quantified by densitometry and plotted versus elution volume. Curves fitted to the data points are shown. Solid black line: FRQ; solid gray line: WC-1. Maximal signals were set equal to 10. Dashed line: FRQ abundance in relation to WC-1. Arrows indicate size standards: thyroglobulin, 669 kDa; apoferritin, 443 kDa; alcohol dehydrogenase, 150 kDa.

(B) Total cell extract (DD25) was subjected to immunoprecipitation with α-WC-1 antibodies. Thirteen percent of the total, 100% of the immunoprecipitate (IP), and 13% of the supernatant (Sup) was analyzed.

is deleted, and in the frq^9 mutant, a truncated, nonfunctional protein is expressed due to a premature stop (Aronson et al., 1994b). Interestingly, WC-1 and WC-2 species with reduced electrophoretic mobility were absent in both strains (Figure 3A, upper panels), suggesting that the phosphorylation status of WCC is dependent on FRQ. To characterize the phosphorylations in more detail, samples were analyzed by 2D gel electrophoresis. We were not able to detect WC-1 on 2D gels. Using cell-free-synthesized radiolabeled WC-1, we found that it did not efficiently enter the isoelectric focusing strips (data not shown). WC-2, which was detected on 2D gels, was phosphorylated at multiple sites in frq^+ (Figure 3A, lower panels). In frq^9, WC-2 was hypophosphor-

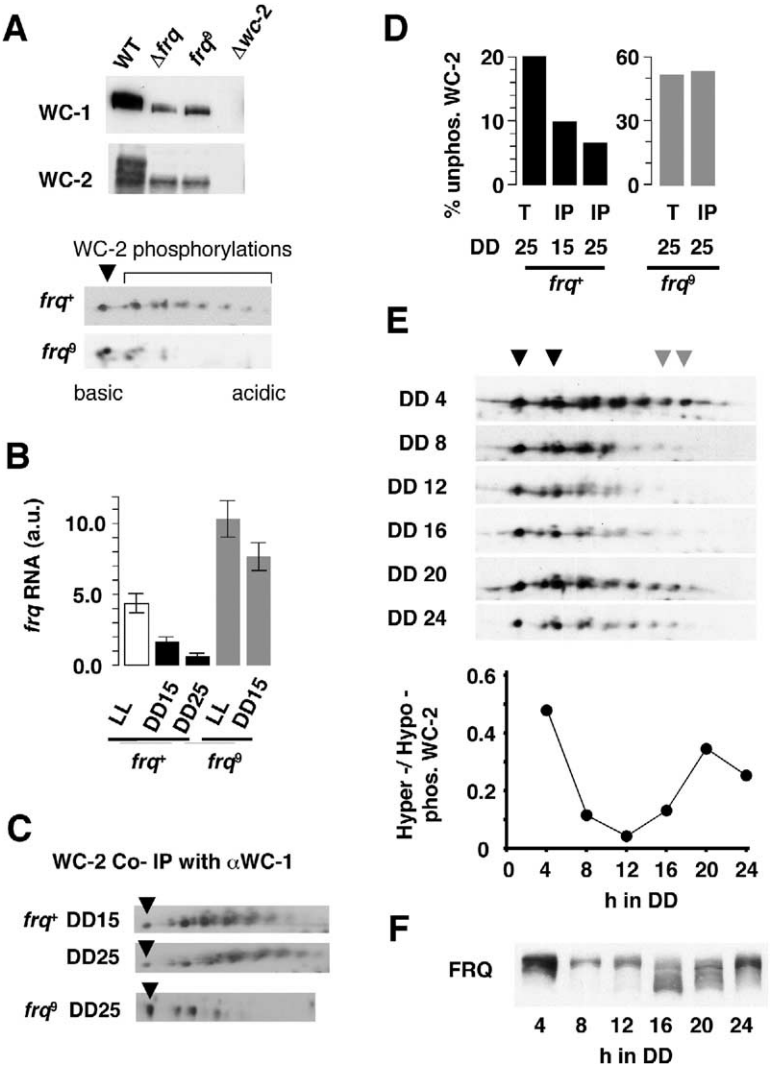

Figure 3. WC-1 and WC-2 Are Expressed and Phosphorylated in FRQ-Dependent Fashion

(A) Phosphorylation status and expression levels of WCC in *frq*$^+$ and *frq*-deficient strains. Upper panels: 1D gel electrophoresis. Δ*wc-2* is shown to control specificity of antibodies. WC-1 is not stably expressed in Δ*wc-2*. Lower panels: Analysis of WC-2 phosphorylation by 2D gel electrophoresis of *frq*$^+$ (DD25) and *frq*^{9} extract.

(B) *frq*^{9} RNA is expressed in a high amount. Total RNA was prepared from *frq*$^+$ and *frq*^{9} grown in constant light (LL) or constant darkness for 15 hr (DD15) and 25 hr (DD25) as indicated. RNA was reverse transcribed and *frq*-RNA abundance relative to *actin* RNA was measured by quantitative real-time PCR. (Error bars: ± SD.)

(C) Phosphorylation status of WC-2 in the WCC. *frq*$^+$ extracts (DD15 and DD25) and *frq*^{9} extracts (DD25) were prepared and WCC was immunoprecipitated with αWC-1 antibodies. WC-2 in the immunoprecipitate was analyzed by 2D gel electrophoresis.

(D) Unphosphorylated WC-2 is underrepresented in WCC of *frq*$^+$ but abundant in WCC of *frq*^{9}. The fraction of unphosphorylated WC-2 in total extracts and in immunopurified WCC was quantified.

(E) Time-of-day-specific phosphorylation status of WC-2. Total protein extracts of cells harvested at the indicated time points were analyzed by 2D gel electrophoresis and Western blotting with α-WC-2 antibodies (upper panels). Two hypophosphorylated WC-2 species (black arrowheads) and two hyperphosphorylated forms (gray arrowheads) were quantified by densitometry. The ratio of hyper- to hypophosphorylated WC-2 is plotted versus the incubation time in DD (lower panel).

(F) Circadian analysis of FRQ. *Neurospora* was harvested at the indicated time points in DD, and FRQ was analyzed by SDS-PAGE and Western blotting.

ylated: about one half was unphosphorylated, and the rest was phosphorylated at one or two sites. It should be pointed out that FRQ^9 did not support hyperphosphorylation of WCC, although nuclear levels of FRQ^9 and FRQ are similar (Figure 1D), suggesting that the C-terminal domain of FRQ is crucial for this function.

To correlate FRQ-dependent phosphorylation with WCC activity, *frq*^{9} and *frq* RNA was measured by quantitative RT-PCR (Figure 3B) and Northern blotting (data not shown). At DD15, *frq* RNA was expressed in a 2.5-fold higher amount than at DD25, reflecting circadian oscillation. Interestingly, the *frq*^{9} RNA level was almost 5-fold higher than the peak level of *frq* RNA (DD15). In *frq*$^+$, WCC is apparently not fully active at DD15, although FRQ levels are very low (circadian trough) and *frq* RNA levels are at a circadian peak. The data suggest that a pool of largely inactive WCC is present in *frq*$^+$ at all times throughout a circadian period. *frq*^{9} and *frq* RNA were both expressed at a higher level in LL than in DD (Figure 3B). Yet *frq*^{9} RNA was expressed in a higher amount than *frq* RNA, demonstrating that FRQ-dependent negative feedback is antagonizing light-induced activation of WCC.

The data suggest that unphosphorylated WCC in *frq*^{9} is transcriptionally more active than hyperphosphorylated WCC in *frq*$^+$. However, the absolute amount of unphosphorylated WC-2 was higher in *frq*$^+$ than in *frq*^{9}. It should be pointed out that ~1/3 of WC-2 is localized in the cytosol (see Figure 1). Immunoprecipitation and subsequent 2D gel analysis and quantification demonstrate that ~10% of WC-2 in complex with WC-1 was unphosphorylated in *frq*$^+$ at DD15 and ~6.5% at DD25, while ~50% was unphosphorylated in *frq*^{9}. (Figures 3C and 3D). Thus, although overall levels of WCC (WC-1) are four to five times lower in *frq*^{9} (Figure 3A and data not shown), there is more unphosphorylated WC-2 in complex with WC-1. Accordingly, the amount of unphosphorylated WC-2 in complex with WC-1 appears to correlate with *frq* transcription.

To investigate whether the phosphorylation status of WCC oscillates in circadian fashion, extracts were prepared at 4 hr intervals from dark-grown *Neurospora* and analyzed by 2D gel electrophoresis. The phosphorylation status of WC-2 was dependent on circadian time (Figure 3E). The fraction of hyper- versus hypophosphorylated WC-2 was lowest at DD12, i.e., at the onset

of *frq* transcription, when FRQ protein levels are low (Figure 3F). It should be noted that the hypophosphorylated WC-2 present throughout the circadian cycle represents predominantly cytosolic WC-2, which is not incorporated into WCC (compare with Figure 3C). The cytosolic fraction of WC-2 is hypophosphorylated at all times (see Figure 1).

A significant fraction of WC-2 was phosphorylated at either time point in DD, while the majority of WC-2 was unphosphorylated in frq^9. This suggests that WCC may not be fully active in frq^+ at any circadian time (see below).

As shown in Figure 3A, the low-mobility form of WC-1 represents a species phosphorylated in an FRQ-dependent manner. When analyzed on 1D gels, the ratio of high- versus low-mobility species of WC-1 appeared to be slightly higher at DD15 than at DD25 (data not shown), suggesting that the phosphorylation status of WC-1 may oscillate with low amplitude.

In summary, a comparison of WCC phosphorylation status and corresponding *frq* RNA levels indicates that the extent of WCC phosphorylation correlates inversely with its activity. In the course of a circadian cycle, the pool of WCC undergoes a change in phosphorylation status. FRQ directly or indirectly promotes phosphorylation of WCC. The hyperphosphorylated pool of WCC in frq^+ displays considerably low activity compared to the activity of hypophosphorylated WCC in frq^9.

Activation of WCC

We then asked whether phosphorylation status and activity of the entire pool of WCC could be manipulated in vivo. If factors establishing WCC phosphorylation (e.g., FRQ, kinases, and phosphatases) were turned over at different rates, inhibition of de novo synthesis of these factors could significantly unbalance the phosphorylation status of WCC. To probe this hypothesis, we used the translational inhibitor cycloheximide (CHX). frq^+ cultures were initially grown in constant light to accumulate high levels of FRQ. Since WCC is stable in the dark (Lee et al., 2000 and data not shown), the cultures were then transferred to the dark (LD transfer) with and without addition of CHX. *frq* RNA amount, phosphorylation status of WCC, and turnover of FRQ were determined over a time course of 16 hr (Figure 4). In the control incubation (–CHX), *frq* RNA levels were low 2 hr after LD transfer, demonstrating that *frq* RNA synthesis was efficiently suppressed via negative feedback of the high amounts of FRQ synthesized during the preceding light incubation (Figures 4A and 4B). *frq* RNA reached a circadian peak at DD16, indicating that the circadian clock was running. In the presence of CHX, *frq* RNA levels were also low at DD2. Subsequently, however, *frq* RNA amounts increased dramatically, reaching a ~40-fold higher level at DD16 compared with –CHX cultures. Since no protein is synthesized in the presence of CHX, the significant increase in *frq* RNA amount must be due to activation of previously synthesized components. Corresponding results were obtained when dark-grown frq^+ was incubated with CHX (see Figure 5C). frq^9 RNA levels are elevated compared to frq^+. When frq^9 was incubated with CHX (Figures 4A and 4B), frq^9 RNA levels remained constant at intermediate level over the entire time period. This indicates that the CHX-dependent increase of *frq* RNA is dependent on functional FRQ and not due to a pleiotropic effect of CHX. This was supported by further controls: no CHX-dependent increase of *frq* RNA amount was observed in a *wc-1*-deficient strain (data not shown). Furthermore, levels of control RNAs (*cyclophilin* RNA and *tim17* RNA) did not increase in the presence of CHX (data not shown). These data demonstrate that the CHX-dependent increase in *frq* RNA is specific and dependent on FRQ and WCC.

We analyzed the phosphorylation status of WC-1 and WC-2 (Figure 4C). Both proteins were dephosphorylated in the presence of CHX. In frq^9, WC-1 was hypophosporylated (high-mobility form) and expressed in a low amount, and its phosphorylation status did not change upon incubation with CHX. Similarly, the phosphorylation status of WC-2 did not change in frq^9 (not shown). Thus, abundance of *frq* and frq^9 RNA correlates with the phosphorylation status of WCC, supporting the hypothesis that the hypophosphorylated form of WCC is transcriptionally more active.

CHX-specific activation of WCC did not correlate with the apparent kinetics of FRQ turnover, which was similar upon LD transfer in presence and absence of CHX (Figure S4 and Görl et al., 2001), suggesting that FRQ may not be the rate-limiting component affected by CHX. However, negative feedback on the *frq* promoter is never complete. Thus, in the absence of CHX, low levels of FRQ are synthesized even when *frq* RNA levels are at trough. If newly synthesized FRQ were active in feedback, the pool of WCC might never become completely activated in the absence of CHX. In contrast, WCC could become fully activated by efficient inhibition of de novo FRQ synthesis.

To test whether tighter repression of FRQ synthesis would lead to more efficient activation of WCC, we expressed in frq^9 a His-tagged version of FRQ (FRQ-His) under control of the *qa-2* promoter, which is tightly regulated by quinic acid (QA). To generate high peak-to-trough oscillation of FRQ, the transformed strain was initially grown in the absence of QA. Then, QA was added to induce synthesis of FRQ-His. After 4 hr, the cells were transferred to growth medium without QA to repress synthesis of FRQ-His and incubated for 16 hr. No FRQ-His was detected prior to addition of QA, demonstrating that the *qa-2* promoter was tightly repressed (Figure 4D). As expected, WC-1 levels were low in the absence of FRQ; WC-1 and WC-2 accumulated in hypophosphorylated form and the mutant frq^9 allele was efficiently transcribed, as measured with a 5′UTR-specific probe absent in the *qa-2*-driven frq^+ allele (Figure 4D). Four hours after addition of QA, FRQ-His was expressed. WC-1 levels were slightly elevated, reflecting that the newly synthesized FRQ started to support accumulation of WC-1 (Lee et al., 2000). Low-mobility forms of WC-1 and WC-2 appeared, and frq^9 RNA was efficiently repressed (Figure 4D). This indicates that low levels of newly synthesized FRQ were active in negative feedback and in triggering phosphorylation of WCC. After transfer to QA-free medium, synthesis of FRQ-His continued for ~4 hr (not shown), and the protein was then degraded during the subsequent period. Low levels of hyperphosphorylated FRQ-His were detected after

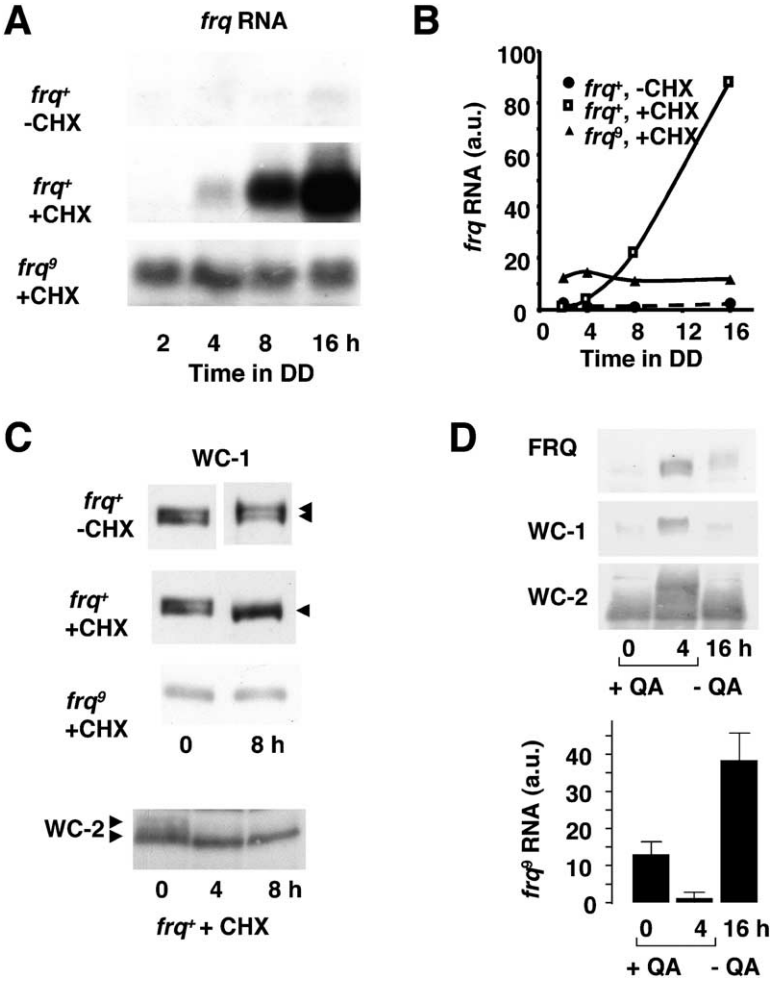

Figure 4. Activation of WCC Correlates with Dephosphorylation

(A) *frq* RNA levels are induced by CHX. Light-grown *frq*$^{+}$ and *frq*^{9} were transferred to darkness in the presence or absence of 10 μg/ml CHX. Samples were harvested at indicated time points, and *frq* RNA was measured by Northern blot analysis.

(B) *frq* RNA amount was quantified and plotted versus incubation period.

(C) Dephosphorylation of WCC is induced by CHX. Protein extracts prepared prior to the addition of CHX (0 hr) and after addition of CHX were analyzed by immunoblotting with antibodies against WC-1 and WC-2.

(D) Pulse of FRQ expression under control of the *qa-2* promoter. *frq*^{9}, *qa*-FRQ-His was grown in 2% glucose medium. 10 mM quinic acid (QA) was added to induce synthesis of His-tagged FRQ. After 4 hr, cells were transferred to QA-free medium (0.1% glucose). Samples were harvested at time 0 hr and 4 hr after induction with QA and 16 hr after transfer. Upper panels: Western blot analysis of FRQ, WC-1, and WC-2. Note that low-mobility (hyperphosphorylated) species of WC-1 and WC-2 appear after induction of FRQ and high-mobility (hypophosphorylated) species after 16 hr incubation without QA. Lower panel: *frq*^{9} RNA was quantified by RT-PCR. A TaqMan probe specific to the 5′ untranslated region of *frq*^{9} was used to discriminate *frq*^{9} RNA (driven by the *frq* promoter) from the functional *frq* gene (ORF only) driven by the *qa-2* promoter. (n = 6; error bars: ± SD.)

16 hr (Figure 4D). WC-1 levels were lower than after FRQ-His induction but slightly higher than initial WC-1 levels. WC-1 and WC-2 were both in hypophosphorylated form. Interestingly, *frq*^{9} RNA levels were 3-fold higher than the initial levels and ~40-fold higher than trough levels after FRQ-His induction. This indicates that a control of FRQ synthesis tighter than in *frq*$^{+}$ produces significant changes in phosphorylation status of WCC and high peak-to-trough ratios of *frq*^{9} RNA. The data strongly suggest that during a circadian cycle in *frq*$^{+}$, FRQ-mediated feedback on WCC activity sets in well before the pool of WCC is fully activated.

Dephosphorylation of WCC Is Dependent on the RGB-1 Regulatory Subunit of PP2A

Recently, Liu and coworkers have shown that expression of *frq* RNA and FRQ protein was reduced in a strain in which RGB-1, a regulatory subunit of PP2A, was inactivated by repeat-induced point mutation (RIP) (Yang et al., 2004). Expression levels of WC-1 were not affected in *rgb-1*^{RIP}. Since these observations are consistent with reduced WCC activity, we compared WCC phosphorylation status in *frq*$^{+}$ and *rgb-1*^{RIP}. About 50% of WC-1 was shifted in electrophoretic mobility in *frq*$^{+}$ (Figure 5A). In contrast, electrophoretic mobility of essentially all WC-1 was reduced in *rgb-1*^{RIP}, indicating that the entire pool of WC-1 was hyperphosphorylated when RGB-1-dependent function of PP2A was compromised. The phosphorylation status of WC-2 was also affected by PP2A (Figure 5B). In addition to un- and monophosphorylated WC-2, two hyperphosphorylated species, comprising ~60% of WC-2, accumulated in *rgb-1*^{RIP}. However, compared to *frq*$^{+}$, the apparent phosphorylation status of WC-2 did not change in circadian fashion in *rgb-1*^{RIP}. Thus, neither did hypophosphorylated WC-2 accumulate at DD15 nor were highly phosphorylated species detected at DD25. The lack of an apparent high-amplitude phosphorylation rhythm mirrors the reported low-amplitude rhythm in *frq* RNA abundance in *rgb-1*^{RIP} (Yang et al., 2004).

To test whether dephosphorylation and activation of WCC are dependent on PP2A, *frq*$^{+}$ and *rgb-1*^{RIP} cultures (DD15) were incubated with CHX. WC-1 was efficiently dephosphorylated after CHX treatment of *frq*$^{+}$ for 4 hr and 8 hr but remained hyperphosphorylated in CHX-treated *rgb-1*^{RIP} (Figure 5A, right panel). *frq* RNA levels increased in CHX-treated *frq*$^{+}$ but not in CHX-treated *rgb-1*^{RIP} (Figure 5C). Together, the data demonstrate that the RGB-1-dependent function of PP2A is crucial for both the phosphorylation status of WCC and the CHX-induced activation of *frq*.

Next, *rgb-1*^{RIP} extract was prepared and WCC was im-

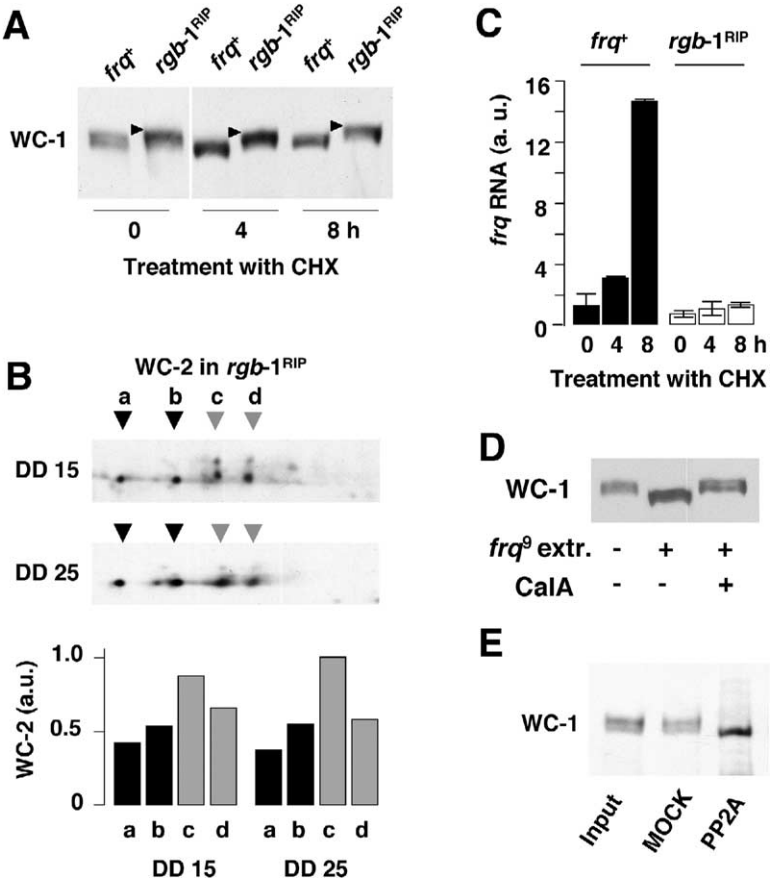

Figure 5. PP2A-Controlled Phosphorylation Status Determines WCC Activity

(A) Phosphorylation status of WC-1 depends on RGB-1, a regulatory subunit of PP2A. *frq*$^{+}$ and *rgb-1*^{RIP} (Fungal Genetic Stock Center) were incubated as indicated without and with CHX, and WC-1 was analyzed. WC-1 remains hyperphosphorylated (arrowhead) in CHX-treated *rgb-1*^{RIP}.

(B) Phosphorylation status of WC-2 is affected by PP2A. *rgb-1*^{RIP} cultures were harvested at DD15 and DD25, extracts were prepared in the presence of phosphatase inhibitors, and WC-2 was analyzed by 2D electrophoresis. Un-, mono-, di-, and triphosphorylated WC-2 species (a–d) were quantified by densitometry (lower panel).

(C) CHX-induced increase in *frq* RNA is dependent on RGB-1. *frq* RNA was quantifified by RT-PCR. (n = 4; error bars: ± SD.)

(D) In vitro dephosphorylation of WC-1 by *frq*^{9} extract. WC-1 was immunoprecipitated from *rgb-1*^{RIP} cell extract. The immunoprecipitate (lane 1) was incubated for 1 hr at 30°C with *frq*^{9} extract (lane 2) or with *frq*^{9} extract and caliculin A (lane 3). Samples were analyzed by Western blotting.

(E) Dephosphorylation of WC-1 by PP2A. WC-1 was immunoprecipitated from total cell extract. The immunoprecipitate (Input) was incubated without (MOCK) or with purified human PP2A AC dimer (Upstate Biotech) for 20 min at 30°C, and samples were analyzed.

munoprecipitated with WC-1-specific antibodies. When the immunopurified WCC was incubated with protein extract prepared from *frq*^{9}, WC-1 was efficiently dephosphorylated, indicating that the *frq*^{9} extract contained a WCC-specific phosphatase activity that was apparently absent in *rgb-1*^{RIP} (Figure 5D). The dephosphorylation was inhibited by caliculin A.

Then, immunoprecipitated WCC was incubated with purified human PP2A (AC dimer). WC-1 (Figure 5E) and WC-2 (data not shown) were dephosphorylated, demonstrating that WCC is a direct substrate of PP2A in vitro.

Finally, a FLAG-tagged version of RGB-1, which was stably expressed in *Neurospora*, accumulated in cytosol and nuclei (Figure S5A), indicating that it assembled with the A and C subunits of PP2A (Virshup, 2000). Its subcellular distribution was independent of FRQ, and it did not coimmunoprecipitate with FRQ (data not shown), suggesting that PP2A function may not be modulated by FRQ. However, the phosphorylation status of WC-2 was slightly shifted toward hypophosphorylation, suggesting that the overexpressed protein was active in promoting dephosphorylation of WC-2 (Figure S5B).

Together, the data demonstrate that CHX-dependent activation of WCC correlates with its dephosphorylation in vivo. CHX-dependent dephosphorylation as well as transcriptional activation of WCC is directly or indirectly dependent on PP2A.

Binding of WCC to the C Box

The analysis of *frq*^{9} in vivo clearly demonstrates that hypophosphorylated WCC is transcriptionally active, but there is only a strong in vivo correlation that hyperphosphorylated WCC is less active. Since these species accumulate only in the presence of functional FRQ, it cannot be rigorously concluded that FRQ, though present in a substoichiometric amount, inactivates WCC by other means. To obtain direct evidence, we studied in vitro binding of WCC to a C box oligonucleotide derived from the *frq* promoter (Froehlich et al., 2003). Nuclear extracts were prepared from *frq*^{9} (DD15) and from *frq*$^{+}$ at DD15 and DD25. The capacity of WCC to bind to a radiolabeled oligonucleotide specific to the C box was then analyzed by electrophoretic mobility shift assay (EMSA). *frq*^{9} nuclear extract efficiently shifted the mobility of the C box oligonucleotide (Figure 6A). *frq*$^{+}$ nuclear extracts prepared at DD15 and DD25 differed slightly in their ability to bind to the C box, but both were significantly less efficient in EMSA than *frq*^{9} extract. This indicates that low amounts of hypophosphorylated WCC present in *frq*^{9} were more active than high amounts of hyperphosphorylated WCC present in *frq*$^{+}$.

If WCC is inactivated by FRQ-dependent phosphorylation rather than by complex formation with FRQ per se, neither addition nor depletion of FRQ should affect binding of WCC to the C box. Thus, we affinity purified FRQ-His, which is active in negative feedback in vivo (see Figure 4D). *frq*^{9} nuclear extract was then incubated with increasing amounts of purified FRQ-His and subjected to EMSA (Figure 6B, left lanes). Addition of FRQ-His in ~40-fold molar excess over WC-1 did not reduce binding of WCC to the C box. The data support that

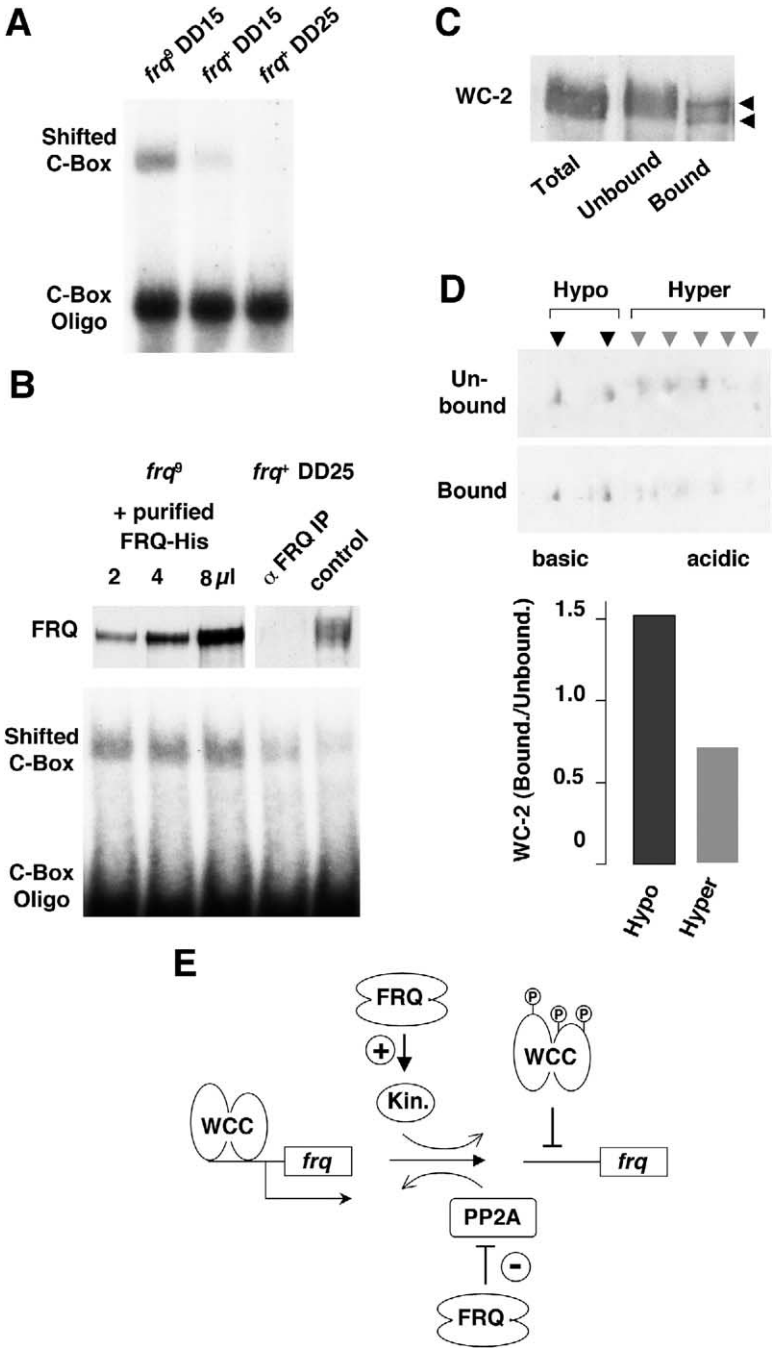

Figure 6. FRQ Does Not Directly Affect WCC Binding to the C Box of the *frq* Promoter

(A) Electrophoretic mobility shift assay (EMSA). A ^{32}P-labeled oligonucleotide corresponding to the C box of the *frq* promoter (Froehlich et al., 2003) was incubated with the indicated nuclear extracts (3 μg).

(B) Addition or depletion of FRQ does not affect binding of WCC to the C box. Purified FRQ-His (top left panel) was added to *frq*^{9} nuclear extract in ~10×, 20×, or 40× excess over WC-1, and EMSA (lower panel) was performed (lanes 1–3). FRQ-depleted DD25 extract and control-treated extract (top right panel) were used for EMSA (lower panel, lanes 4 and 5).

(C and D) Hypophosphorylated WCC binds preferentially to the C box. A C box oligonucleotide carrying a sulfhydryl at the 5′ end of the upper strand was coupled to SulfoLink resin. *frq*$^+$ extract (LL) was mixed with 100 μg/ml poly dI/dC and passed over the C box affinity column. WC-2 was analyzed by 1D (C) and 2D (D) gel electrophoresis. The fraction of un- and monophosphorylated WC-2 (Hypo, black arrowheads) and the fraction of hyperphosphorylated WC-2 (Hyper, gray arrowheads) were quantified by densitometry. The ratio of bound to unbound WC-2 is shown in the lower panel.

(E) Model of FRQ-dependent negative feedback on WCC. Hypophosphorylated WCC binds to the C box in the *frq* promoter and activates transcription (left), while hyperphosphorylated WCC binds with reduced affinity and is transcriptionally inactive (right). WCC is inactivated via phosphorylation by unknown kinase and is activated by dephosphorylation requiring PP2A directly or indirectly. FRQ promotes inactivation of WCC by activating phosphorylation or inhibiting dephosphorylation of WCC.

WCC is not inactivated by direct complex formation with FRQ.

According to our hypothesis, depletion of FRQ should not restore impaired binding to the C box of phosphorylated WCC. To test this prediction, FRQ was immunodepleted from *frq*$^+$ DD25 extract. Depletion of FRQ neither increased nor decreased the interaction of WCC with the C box (Figure 6B, right lanes). Thus, at DD25, WCC is mostly incapable of binding to the C box, and FRQ is not directly required to maintain WCC in an inactive state.

Then, to directly compare the binding activity of hyper- and hypophosphorylated WCC, we prepared an affinity resin by coupling a sulfhydrylated C box oligonucleotide to an iodoacetate resin. *frq*$^+$ extract was then passed over the affinity column. Poly dI/dC was included to reduce unspecific binding. Under the conditions used (100 mM KCl), about 40% of WCC bound to the C box affinity resin. As shown by 1D and 2D gel electrophoresis and quantification (Figures 6C and 6D), hypophosphorylated WC-2 species were enriched in the bound fraction, demonstrating that hyperphosphorylated WCC is less active in binding to the C box.

In summary, the data indicate that binding of WCC to

the C box depends on its phosphorylation status and is independent of presence or absence of FRQ.

Discussion

The *Neurospora* clock protein FRQ feedback-regulates its own mRNA synthesis by inhibiting its transcriptional activator WCC. Here we have analyzed the mechanism of negative feedback. We show that FRQ and WCC, though expressed in similar abundance, localize to different subcellular compartments. WCC is highly enriched in nuclei, while FRQ localizes predominantly to the cytosolic compartment, resulting in excess of WCC over nuclear FRQ even at times of day when *frq* RNA synthesis is maximally repressed. Furthermore, the vast majority of WCC is not interacting with FRQ. Small amounts of WCC were found in a complex with FRQ, in agreement with earlier reports (Denault et al., 2001; Merrow et al., 2001; Yang et al., 2002; Cheng et al. 2003; Cheng et al., 2005), but this cannot account for the inactivity of the bulk of WCC. Our data present quantitative and qualitative evidence that the activity of WCC is regulated by a mechanism different from direct stable complex formation with FRQ.

We show that the phosphorylation status of WCC is dependent on FRQ. Both components, WC-1 and WC-2, are phosphorylated. Recently, five phosphorylation sites of WC-1 were identified (He et al., 2005). Phosphorylation of these sites negatively regulates the function of WC-1. Whether these are the sites that are phosphorylated in an FRQ-dependent manner remains to be investigated. Phosphorylation sites in WC-2 are not known. The phosphorylation status of WC-2 oscillates in the course of a circadian cycle and correlates with the function of WCC as transcriptional activator: hypophosphorylated WCC efficiently binds to the C box of the *frq* promoter in vitro and supports transcription of *frq* RNA in vivo, while hyperphosphorylated WCC binds to the C box with reduced affinity and does not efficiently activate transcription. Impaired binding of hyperphosphorylated WCC is independent of the presence of FRQ, demonstrating that hyperphosphorylation interferes with DNA binding. Additionally, distinct phosphorylation steps could independently contribute to inactivation of WCC by different molecular mechanisms similar to those leading to inactivation of the transcription factor Pho2/Pho4 of *S. cerevisiae* (Carroll and O'Shea, 2002; Byrne et al., 2004). In this system, five distinct phosphorylations of Pho4 interfere with its transcriptional activity, inhibit complex formation with Pho2, promote nuclear export, and block nuclear import.

FRQ-dependent phosphorylation leads to inactivation of WCC. Since light-induced phosphorylation of WCC leads to activation, the corresponding phosphorylation sites must be distinct. We do not know whether WCC is also activated by phosphorylation at distinct sites in DD. Two-dimensional gel electrophoresis analyzes the overall number of phosphorylations but does not discriminate between phosphorylation at different sites. If WCC would be activated and inactivated via phosphorylation, the apparent circadian oscillation of the overall phosphorylation status of WCC would not reflect the dynamics of phosphorylation at distinct sites.

Together, observations in vivo and in vitro demonstrate that FRQ controls WCC activity by modulating its phosphorylation status. The small fraction of WCC that is found in complex with FRQ suggests a "hit-and-run" mode of WCC inactivation. Since FRQ is apparently not interacting with RGB-1 and since WCC is hypophosphorylated in the absence of FRQ, it may transiently recruit or activate a kinase and thereby facilitate phosphorylation of WCC. By promoting phosphorylation of WCC in rhythmic fashion, the clock protein FRQ can be viewed as a circadian cyclin, functionally equivalent to a cyclin regulating its molecular targets via cyclin-dependent kinase (CDK), similar to Pho80/Pho85, a yeast cyclin/CDK complex that inactivates the transcription factor Pho2/Pho4 (Carroll and O'Shea, 2002; Byrne et al., 2004).

FRQ, though preferentially localized in the cytoplasm, contains a nuclear localization sequence (NLS) that is essential for clock function (Luo et al., 1998). Compatible with a hit-and-run mechanism, FRQ may shuttle components between cytosol and nuclei that regulate phosphorylation of WCC. Since subcellular distribution of RGB-1 was not dependent on FRQ, it may transport a kinase into the nucleus. The C-terminally truncated FRQ^9 protein is enriched in nuclei. Yet WCC is hypophosphorylated in frq^9, suggesting that the C-terminal domain of FRQ is required for both subcellular localization or shuttling of FRQ and phosphorylation of WCC. FRQ is in a complex with CK-1a (Görl et al., 2001), a homolog of mammalian CKI$\epsilon\delta$ and *Drosophila* Double-time (DBT). It remains to be investigated whether FRQ-associated CK-1a phosphorylates WCC.

In the Wnt/β-catenin signaling pathway, CKI$\epsilon\delta$ was shown to collaborate with PP2A (Gao et al., 2002; Swiatek et al., 2004). We show that PP2A with its regulatory subunit RGB-1 is required for establishing the phosphorylation status of WCC in vivo. CHX-induced dephosphorylation of WCC and activation of *frq* transcription is also dependent on functional RGB-1. It seems likely that WCC is directly dephosphorylated and activated by PP2A/RGB-1. However, an indirect mechanism cannot be excluded, and other phosphatases may contribute to the phosphorylation status of WCC.

Oscillation of *frq* abundance is driven by a pool of WCC that is only partially active even when *frq* RNA levels are at their circadian peak. WCC was fully activated when FRQ expression under control of the heterologous *qa-2* promoter was tightly repressed or when FRQ synthesis was inhibited by CHX. Activation was accompanied by extensive dephosphorylation of WCC and resulted in ~40-fold activation of *frq* transcription. Apparently, in constant conditions, FRQ-mediated negative feedback (WCC phosphorylation) already sets in before the pool of WCC is fully activated, maintaining WCC in a mostly inactive form throughout the entire circadian cycle.

Recruiting active WCC primarily from a large pool of inactive protein rather than by de novo synthesis could contribute to robustness of the circadian oscillator. De novo biogenesis of WCC would primarily serve the purpose of replenishing the WCC pool. In accordance, WC-2 is expressed in excess and at constant levels, while WC-1 levels oscillate supported by FRQ (Lee et al., 2000; Cheng et al., 2001; Görl et al., 2001). However,

the peak of WC-1 expression (CT14–19) does not coincide with the peak of *frq* RNA (CT4), suggesting that FRQ supports expression of inactive WCC to replenish the pool.

In summary, our data suggest that FRQ feedback-regulates its own RNA synthesis by antagonizing PP2A-dependent activation of WCC (Figure 6E). A post-translational feedback loop promoting rhythmic phosphorylation of KaiC is critical in the circadian system of cyanobacteria (Tomita et al., 2005). It is not known whether corresponding mechanisms of negative feedback contribute to clock function in other circadian systems, but reported data seem compatible with such a mode of posttranslational regulation in mice and flies.

Mouse CLK/BMAL1 is phosphorylated and interacts with PER/CRY complexes (Lee et al., 2001). BMAL1 appears to be negatively regulated by MAP kinase (Sanada et al., 2002). The fraction of CLK/BMAL1 interacting in vivo with PER/CRY has not yet been determined. CLK/BMAL1 activates and PER/CRY inhibits transcription of *per2*, *cry*, and *rev-erbα* genes, leading to rhythmic expression of their mRNAs. Yet the circadian phases of accumulation of these mRNAs differ by up to 11 hr, such that peak levels of the inhibitor PER/CRY coincide with trough levels of *rev-erbα* RNA and almost peak levels of *per2* and *cry* RNA (for review, see Gachon et al., 2004). A simple mechanism of feedback cannot fully account for these observations.

Drosophila PER/TIM inhibits DNA binding of CLK/CYC (Lee et al., 1999). Phosphorylation of CLK/CYC oscillates in circadian fashion (Lee et al., 1998, 1999; Kim et al., 2002). PP2A controls PER stability in *Drosophila* (Sathyanarayanan et al., 2004), but a role in regulation of CLK/CYC was not investigated. DBT collaborates with CKII to potentiate PER-dependent transcriptional repression of CLK/CYC (Nawathean and Rosbash, 2004), but it is not known whether repression requires phosphorylation of CLK/CYC.

Thus, although the role of phosphorylation of CLK/CYC and CLK/BMAL1 remains to be determined, modulation of transcription-factor activity by a mechanism similar to that described here for WCC could also contribute to clock function in these circadian systems.

Experimental Procedures

Strains and Growth Conditions

Neurospora strains used in this study (*frq*$^{+}$, *frq*^{9}, *frq*^{10}, and Δ*wc-2*) carried the *bd* mutation. Standard growth medium contained 2% glucose, 0.5% L-arginine, 1× Vogel's, and 10 ng/ml biotin.

Protein Analysis

Extraction of *Neurospora* protein and subcellular fractionation was performed as described (Luo et al., 1998; Görl et al., 2001). For 2D gel analysis, phosphatase inhibitors were added: 30 mM Na pyrophosphate, 20 mM Na phosphate, 5 mM EDTA, 400 nM okadaic acid, 20 mM caliculin, and 2 mM vanadate. Nuclear extracts were prepared by incubating nuclei at 4°C under shaking for 30 min in protein extraction buffer (50 mM HEPES [pH 7.4], 10% glycerol, 137 mM NaCl, 5 mM EDTA, 1 mM phenylmethyl sulfonyl fluoride, 1 μg/ml leupeptin, 1 μg/ml pepstatin A). Western blotting was performed as described (Görl et al., 2001). Enhanced chemiluminescence signals were detected with either X-ray films or a FluorS-Max imager (Bio-Rad). Series of exposures in the range of 5 s to 30 min were generated. Quantification was performed using the QuantityOne software (Bio-Rad).

Immunoprecipitation

Antibody was prebound to protein A-Sepharose beads (30 μl) for 2 hr at room temperature. Beads were washed three times with TBS, and 1.5 mg of protein extract in 500 μl extraction buffer was added. Samples were incubated under rotation for 4–16 hr at 4°C.

Analysis of Protein Complexes by Gel Filtration Chromatography

Protein extracts (12 mg/ml) were incubated for 30 min at 4°C with 200 μg/μl DNaseI, 100 μg/μl RNaseA, 10 μM distamycin, and 5 mM $MgCl_2$ in a total volume of 600 μl Superose 6 buffer (25 mM HEPES [pH 7.4], 1% glycerol, 137 mM NaCl, 1mM EDTA). After a clarifying spin (20 min; 45,000 rpm TLA55), 500 μl were loaded on a Superose 6 column (Amersham). Chromatography was performed at 4°C (0.3 ml/min) with an Äkta-Explorer system (Amersham). Fractions (500 μl) were collected and subjected to TCA precipitation, SDS-PAGE, and Western blotting.

Two-Dimensional Gel Electrophoresis

Protein extracts were denaturated (7 M urea, 2 M thiourea, 4% CHAPS, 40 mM Tris, 1% DTT, 0.5% Servalyte 3-10, and Roche protease inhibitor cocktail complete plus EDTA) and loaded on ReadyStrip IPG strips (17 cm [pH 4–7], Bio-Rad). Strips were rehydrated for 12 hr and isoelectric focusing (IEF) was performed in a Protean IEF system (Bio-Rad) with 50,000V × hr. Prior to two-dimensional analysis by SDS-PAGE, strips were soaked (2 × 15 min) in 6 M urea, 30% glycerol, 2% SDS, 0.39 M Tris-HCl [pH 8.8] containing 0.001% DTT and 0.00046% iodoacetamide and subjected to SDS-PAGE.

RNA Analysis

RNA was prepared and analyzed by quantitative real-time PCR (RT-PCR) or Northern blotting essentially as described (Merrow et al., 2001; Görl et al., 2001): cDNA was synthesized from 2 μg DNase-treated total RNA using the SuperscriptII RT system (Invitrogen) and random hexamer primers. *frq* and *actin* cDNA was detected by RT-PCR (ABI-Prism 7000, Applied Biosystems) using TaqMan probes (Görl et al., 2001). Triplicate reactions (25 μl) containing cDNA equivalent to 0.1 μg RNA were analyzed.

Electrophoretic Mobility Shift Assay (EMSA)

EMSA of [γ-^{32}P]ATP-labeled double-stranded C box oligonucleotide was performed as described (Froehlich et al., 2002). Eighteen fentomoles of purified C box oligonucleotide and 3 μg of nuclear extract were incubated on ice for 30 min. One microgram of poly dI/dC was used as unspecific competitor.

C Box Affinity Chromatography

A double-stranded C box oligonucleotide was synthesized, and the upper strand was derivatized with a 5′ sulfhydryl: 5′-SH-GTGCCC GAGGCGTCCTGATGCCGCTGCAAGACCGAGACGCTGCAAAATTG AGATCTA.

Six nanomoles of double-stranded SH-C box oligonucleotide was coupled to 1 ml SulfoLink matrix (Pierce). The C box affinity resin was incubated with 1.5 mg protein extract in 1 ml EMSA buffer (Froehlich et al., 2002), 100 mM KCl, 0.1 mg/ml poly dI/dC, and phosphatase and protease inhibitors for 15 min rotating and an additional 15 min resting at RT. The resin was then washed with 2 ml buffer and eluted with EMSA buffer containing 1 M KCl.

Supplemental Data

Supplemental Data include five figures and can be found with this article online at http://www.cell.com/cgi/content/full/122/2/235/DC1/.

Acknowledgments

We thank J.J. Loros and J.C. Dunlap for kindly providing Δ*wc-1* and Δ*wc-2* and J. Payk for excellent technical assistance. This work was supported by grants from Deutsche Forschungsgemeinschaft (BR 1375-1 and SFB 638) and from Alexander von Humboldt-Stiftung to K.K.

Received: July 28, 2004
Revised: March 8, 2005
Accepted: May 30, 2005
Published: July 28, 2005

References

Allada, R., Emery, P., Takahashi, J.S., and Rosbash, M. (2001). Stopping time: the genetics of fly and mouse circadian clocks. Annu. Rev. Neurosci. *24*, 1091–1119.

Aronson, B.D., Johnson, K.A., Loros, J.J., and Dunlap, J.C. (1994a). Negative feedback defining a circadian clock: autoregulation of the clock gene *frequency*. Science *263*, 1578–1584.

Aronson, B.D., Johnson, K.A., and Dunlap, J.C. (1994b). Circadian clock locus *frequency*: protein encoded by a single open reading frame defines period length and temperature compensation. Proc. Natl. Acad. Sci. USA *91*, 7683–7687.

Bell-Pedersen, D., Shinohara, M.L., Loros, J.J., and Dunlap, J.C. (1996). Circadian clock-controlled genes isolated from *Neurospora crassa* are late night- to early morning-specific. Proc. Natl. Acad. Sci. USA *93*, 13096–13101.

Byrne, M., Miller, N., Springer, M., and O'Shea, E.K. (2004). A distal, high-affinity binding site on the cyclin-CDK substrate Pho4 is important for its phosphorylation and regulation. J. Mol. Biol. *335*, 57–70.

Carroll, A.S., and O'Shea, E.K. (2002). Pho85 and signaling environmental conditions. Trends Biochem. Sci. *27*, 87–93.

Cheng, P., Yang, Y., and Liu, Y. (2001). Interlocked feedback loops contribute to the robustness of the *Neurospora* circadian clock. Proc. Natl. Acad. Sci. USA *98*, 7408–7413.

Cheng, P., Yang, Y., Gardner, K.H., and Liu, Y. (2002). PAS domain-mediated WC-1/WC-2 interaction is essential for maintaining the steady-state level of WC-1 and the function of both proteins in circadian clock and light responses of *Neurospora*. Mol. Cell. Biol. *22*, 517–524.

Cheng, P., Yang, Y., Wang, L., He, Q., and Liu, Y. (2003). WHITE COLLAR-1, a multifunctional *Neurospora* protein involved in the circadian feedback loops, light sensing, and transcription repression of *wc*-2. J. Biol. Chem. *278*, 3801–3808.

Cheng, P., He, Q., He, Q., Wang, L., and Liu, Y. (2005). Regulation of the *Neurospora* circadian clock by an RNA helicase. Genes Dev. *19*, 234–241.

Correa, A., Lewis, Z.A., Greene, A.V., March, I.J., Gomer, R.H., and Bell-Pedersen, D. (2003). Multiple oscillators regulate circadian gene expression in *Neurospora*. Proc. Natl. Acad. Sci. USA *100*, 13597–13602.

Denault, D.L., Loros, J.J., and Dunlap, J.C. (2001). WC-2 mediates WC-1-FRQ interaction within the PAS protein-linked circadian feedback loop of *Neurospora*. EMBO J. *20*, 109–117.

Dunlap, J.C. (1999). Molecular bases for circadian clocks. Cell *96*, 271–290.

Froehlich, A.C., Liu, Y., Loros, J.J., and Dunlap, J.C. (2002). White Collar-1, a circadian blue light photoreceptor, binding to the frequency promoter. Science *297*, 815–819.

Froehlich, A.C., Loros, J.J., and Dunlap, J.C. (2003). Rhythmic binding of a WHITE COLLAR-containing complex to the frequency promoter is inhibited by FREQUENCY. Proc. Natl. Acad. Sci. USA *100*, 5914–5919.

Gachon, F., Nagoshi, E., Brown, S.A., Ripperger, J., and Schibler, U. (2004). The mammalian circadian timing system: from gene expression to physiology. Chromosoma *113*, 103–112.

Gao, Z.H., Seeling, J.M., Hill, V., Yochum, A., and Virshup, D.M. (2002). Casein kinase I phosphorylates and destabilizes the beta-catenin degradation complex. Proc. Natl. Acad. Sci. USA *99*, 1182–1187.

Görl, M., Merrow, M., Huttner, B., Johnson, J., Roenneberg, T., and Brunner, M. (2001). A PEST-like element in FREQUENCY determines the length of the circadian period in *Neurospora crassa*. EMBO J. *20*, 7074–7084.

He, Q., Cheng, P., Yang, Y., Wang, L., Gardner, K.H., and Liu, Y. (2002). White collar-1, a DNA binding transcription factor and a light sensor. Science *297*, 840–843.

He, Q., Shu, H., Cheng, P., Chen, S., Wang, L., and Liu, Y. (2005). Light-independent phosphorylation of WHITE COLLAR-1 regulates its function in the *Neurospora* circadian negative feedback loop. J. Biol. Chem. *280*, 17526–17532. Published online February 24, 2005. 10.1074/jbc.M414010200

Kim, E.Y., Bae, K., Ng, F.S., Glossop, N.R.J., Hardin, P.E., and Edery, I. (2002). Drosophila Clock protein is under posttranscriptional control and influences light-induced activity. Neuron *34*, 69–81.

Lee, C., Bae, K., and Edery, I. (1998). The *Drosophila* CLOCK protein undergoes daily rhythms in abundance, phosphorylation, and interactions with the PER-TIM complex. Neuron *21*, 857–867.

Lee, C., Bae, K., and Edery, I. (1999). PER and TIM inhibit the DNA binding activity of a Drosophila CLOCK-CYC/dBMAL1 heterodimer without disrupting formation of the heterodimer: a basis for circadian transcription. Mol. Cell. Biol. *19*, 5316–5325.

Lee, K., Loros, J.J., and Dunlap, J.C. (2000). Interconnected feedback loops in the *Neurospora* circadian system. Science *289*, 107–110.

Lee, C., Etchegaray, J.P., Cagampang, F.R., Loudon, A.S., and Reppert, S.M. (2001). Posttranslational mechanisms regulate the mammalian circadian clock. Cell *107*, 855–867.

Lee, K., Dunlap, J.C., and Loros, J.J. (2003). Roles for WHITE COLLAR-1 in circadian and general photoperception in *Neurospora crassa*. Genetics *163*, 103–114.

Linden, H., and Macino, G. (1997). White collar-2, a partner in blue-light signal transduction, controlling expression of light-regulated genes in *Neurospora crassa*. EMBO J. *16*, 98–109.

Luo, C., Loros, J.J., and Dunlap, J.C. (1998). Nuclear localization is required for function of the essential clock protein FRQ. EMBO J. *17*, 1228–1235.

Merrow, M., Franchi, L., Dragovic, Z., Görl, M., Johnson, J., Brunner, M., Macino, G., and Roenneberg, T. (2001). Circadian regulation of the light input pathway in *Neurospora crassa*. EMBO J. *20*, 307–315.

Nawathean, P., and Rosbash, M. (2004). The doubletime and CKII kinases collaborate to potentiate Drosophila PER transcriptional repressor activity. Mol. Cell *13*, 213–223.

Nowrousian, M., Duffield, G.E., Loros, J.J., and Dunlap, J.C. (2003). The frequency gene is required for temperature-dependent regulation of many clock-controlled genes in *Neurospora crassa*. Genetics *164*, 923–933.

Reppert, S.M., and Weaver, D.R. (2002). Coordination of circadian timing in mammals. Nature *418*, 935–941.

Roenneberg, T., and Merrow, M. (2003). The network of time: understanding the molecular circadian system. Curr. Biol. *13*, R198–R207.

Sanada, K., Okano, T., and Fukada, Y. (2002). Mitogen-activated protein kinase phosphorylates and negatively regulates basic helix-loop-helix-PAS transcription factor BMAL1. J. Biol. Chem. *277*, 267–271.

Sathyanarayanan, S., Zheng, X., Xiao, R., and Seghal, A. (2004). Posttranslational regulation of *Drosophila* PERIOD protein by protein phosphatase 2A. Cell *116*, 603–615.

Schibler, U., and Sassone-Corsi, P. (2002). A web of circadian pacemakers. Cell *111*, 919–922.

Schwerdtfeger, C., and Linden, H. (2000). Localization and light-dependent phosphorylation of white collar 1 and 2, the two central components of blue light signaling in *Neurospora crassa*. Eur. J. Biochem. *267*, 414–422.

Stanewsky, R. (2003). Genetic analysis of the circadian system in Drosophila melanogaster and mammals. J. Neurobiol. *54*, 111–147.

Swiatek, W., Tsai, I.C., Klimowski, L., Pepler, A., Barnette, J., Yost, H.J., and Virshup, D.M. (2004). Regulation of casein kinase I epsilon activity by Wnt signaling. J. Biol. Chem. *279*, 13011–13017.

Talora, C., Franci, L., Linden, H., Ballario, P., and Macino, G. (1999).

Role of white collar-1-white collar-2 complex in blue-light signal transduction. EMBO J. *18*, 4961–4968.

Tomita, J., Nakajima, M., Kondo, T., and Iwasaki, H. (2005). No transcription-translation feedback in circadian rhythm of KaiC phosphorylation. Science *307*, 251–254.

Virshup, D.M. (2000). Protein phosphatase 2A: a panoply of enzymes. Curr. Opin. Cell Biol. *12*, 180–185.

Yang, Y., Cheng, P., Zhi, G., and Liu, Y. (2001). Identification of a calcium/calmodulin-dependent protein kinase that phosphorylates the *Neurospora* circadian clock protein FREQUENCY. J. Biol. Chem. *276*, 41064–41072.

Yang, Y., Cheng, P., and Liu, Y. (2002). Regulation of the *Neurospora* circadian clock by casein kinase II. Genes Dev. *16*, 994–1006.

Yang, Y., Cheng, P., He, Q., Wang, L., and Liu, Y. (2003). Phosphorylation of FREQUENCY protein by casein kinase II is necessary for the function of the Neurospora circadian clock. Mol. Cell. Biol. *23*, 6221–6228.

Yang, Y., He, Q., Cheng, P., Wrage, P., Yarden, O., and Liu, Y. (2004). Distinct roles for PP1 and PP2A in the Neurospora circadian clock. Genes Dev. *18*, 255–260.

Yatzkan, E., and Yarden, O. (1999). The B regulatory subunit of protein phosphatase 2A is required for completion of macroconidiation and other developmental processes in *Neurospora crassa*. Mol. Microbiol. *31*, 197–209.

Young, M.W., and Kay, S.A. (2001). Time zones: a comparative genetics of circadian clocks. Nat. Rev. Genet. *2*, 702–715.

Zhu, H., Nowrousian, M., Kupfer, D., Colot, H.V., Berrocal-Tito, G., Lai, H., Bell-Pedersen, D., Roe, B.A., Loros, J.J., and Dunlap, J.C. (2001). Analysis of expressed sequence tags from two starvation, time-of-day-specific libraries of *Neurospora crassa* reveals novel clock-controlled genes. Genetics *157*, 1057–1065.